Journal of Materials Chemistry C

Accepted Manuscript

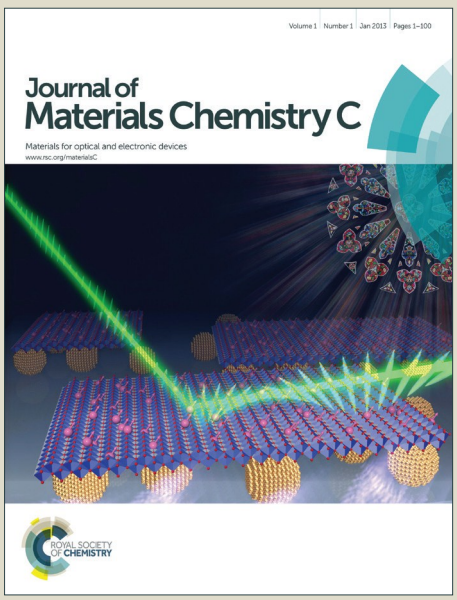

ROYAL SOCIETY OF CHEMISTRY

www.rsc.org/materialsC

Enhanced high temperature thermoelectric response of sulphuric acid treated conducting polymer thin films

S.R. Sarath Kumar,* Narendra Kurra,* and H.N. Alshareef[1]
Materials Science and Engineering, King Abdullah University of Science and Technology (KAUST), Thuwal-23955-6900, Saudi Arabia.

We report the high temperature thermoelectric properties of solution processed untreated and sulphuric acid treated poly(3,4-ethylenedioxythiophene):poly(4-styrenesulfonate) (or PEDOT:PSS) films. The acid treatment is shown to simultaneously enhance the electrical conductivity and Seebeck coefficient of the metal-like films, resulting in a five-fold increase in thermoelectric power factor (from 0.01 to 0.052 W/m.K) at 460 K, compared to the untreated film. By using atomic force micrographs, Raman and impedance spectra and using a series heterogeneous model for electrical conductivity, we demonstrate that acid treatment results in the removal of PSS from the films, leading to the quenching of accumulated charge-induced energy barriers, facilitating metal-like conduction. The continuous removal of PSS and changes in morphology of the PEDOT grains upon acid treatment may alter the local band structure of PEDOT:PSS, in such a way as to simultaneously enhance the Seebeck coefficient.

[1] Corresponding author: husam.alshareef@kaust.edu.sa
* These authors contributed equally to the work.

1. Introduction

Conducting polymers (CPs), also known as synthetic metals, have become attractive due to their intriguing optical and electronic properties.[1-4] Solution processability, flexibility, light-weight and cost-effectiveness are the key attributes of CPs which make them compatible in various applications.[4-6] For example, CPs can be used as both active and passive materials in organic electronics[6, 7] and chemical or electrochemical sensors[8], owing to the tunable electrical conductivity and surface properties.[9] Intrinsic low thermal conductivity of CPs (at least one order of magnitude lower to inorganic materials) due to nanostructured interfaces or grains is one of the potential aspects in exploring CPs as thermoelectric materials.[2, 10-14]

Several CPs such as polyaniline (PANI), polypyrrole (PPY), polyphenylvinylene (PPV), polycarbazole (PC), and polyalkylthiophene have been tested for thermoelectric property; they have low electrical conductivity and hence their potential as a thermoelectric material is limited.[10] In order to enhance the thermoelectric properties of CPs, a wide variety of conducting fillers such as graphene, CNTs and composites with semiconducting inorganic materials have been introduced into the polymer matrix.[15] Poly(3, 4-ethylenedioxythiophene), popularly known as PEDOT, is a good choice as a polymer matrix due to its high environmental stability and electrical conductivity, in its oxidized state.[16, 17] PEDOT:PSS is a complex of PEDOT and poly(4-styrenesulfonate), in which hydrophilic PSS component acts as a soluble matrix for PEDOT domain, while also introducing a counter ion effect which helps maintain the electrical neutrality of the complex. Thin films obtained from the aqueous dispersion of PEDOT:PSS consist of conducting PEDOT grains surrounded by insulating PSS shells.[17] Pristine PEDOT:PSS films tend to exhibit low chain alignment with the presence of excess PSS.[1-3] This kind of morphological features result in a lower electrical conductivity of 1-10 S/cm. Typical

enhancement in the conductivity upon treatment has been explained through the removal of PSS components while forming extended conducting grains of PEDOT.[17] There have been efforts in controlling the doping level of PEDOT chemically and electrochemically to optimize its thermoelectric performance. Treatment with organic solvents such as DMSO and ethylene glycol has been shown to enhance the electrical conductivity of PEDOT:PSS films.[16] Blends of PEDOT:PSS with other organic and inorganic compounds have resulted in enhanced thermoelectric response.[18-21] The effect of humidity on the thermoelectric performance of PEDOT:PSS has been studied wherein an apparent increase in the Seebeck coefficient was observed, and has been attributed to the morphological change after water absorption or electrochemical reaction of PEDOT in air.[22] It has been demonstrated that Seebeck coefficient of PEDOT can be enhanced by chemical reduction[23] and exposure to a reducing environment.[24] Post-deposition treatment of PEDOT:PSS films with acids such as H_2SO_4 has been demonstrated to be effective in enhancing electrical conductivity.[25, 26] Recently, Mengistie *et al.*, have investigated the thermoelectric performance of PEDOT:PSS papers by enhancing the electrical conductivity via post treatment with organic solvents and formic acid.[27] Also, available literature on this important class of developing thermoelectric material is limited to studies at room temperature. To the best of our knowledge, there has been only one previous report on the high temperature thermoelectric properties on PEDOT based films[28] and none on PEDOT:PSS film. Hence, it is worthwhile to investigate the high temperature properties (but not exceeding 500 K) of PEDOT:PSS based thermoelectric films with addition of methanol, followed by acid treatment, to explore both the effectiveness of these materials at elevated temperature and the highest temperature of stable operation; both should help expand the scope of polymer thermoelectrics. With this view, here we report the thermoelectric property of PEDOT:PSS films

in a post-deposition acid treatment process, in the temperature range 300-520 K, to explore the potential of this important polymer as a viable thermoelectric material at room temperature and high temperatures.

2. Experimental

In the present work, chemicals were used as received without further purification. PEDOT:PSS dispersion (PH1000, Clevios^{TM}) in water was employed as a conducting polymer solution. Films formed directly from the as received solution is represented as 'pristine'. 30 vol% of methanol was added to the water dispersion of PEDOT:PSS, in order to increase the wettability over the surface of the glass substrate. Quality of the PEDOT:PSS films seems much better after adding methanol when compared to pristine water dispersion. Thick films (of thickness ~3 μm) of PEDOT:PSS were obtained by drop casting 10 μL of the solution over cleaned 1 × 1 cm square glass substrates (Fischer Scientific), followed by drying on a hot plate at 120 ºC for 15 minutes. Films thus formed are represented as 'un-treated'. The films were then subjected to a surface treatment with 1M H_2SO_4 (Sigma-Aldrich), at 140 ºC for different duration (15 minutes, 2 and 4 h) and then washed with DI water followed by drying in a fume hood at room temperature, and are represented as 'acid-treated'. Surface morphology, microstructure and cross-sectional images were obtained using scanning electron microscope (SEM) (Nova Nano 630 instrument, FEI Co., The Netherlands). Energy-dispersive spectroscopy (EDS) analysis was performed with an EDAX Genesis instrument (Mahwah, NJ) attached to the SEM column. The thickness of the films was measured using a Veeco Dektak 150 surface profilometer. Raman spectra were recorded using a micro-Raman spectrometer (LabRAM ARAMIS, Horiba-Jobin Yvon), with notch filters cutting at 100 cm^{-1} and using a cobalt laser (473 nm, 5 mW at source)

with a laser spot size of 1.5 μm. AFM imaging (MFP-3D, Asylum Research) was done using Si probes (model, RTESPA, spring constant 40 N/m) in tapping mode and images were processed using WSXM software.[29] X-ray diffraction (XRD) was used to investigate the evolution of PEDOT fibrous morphology up on acid treatment (D8 Advance System from Bruker Corporation, equipped with Cu Kα X-ray source, λ = 0.15406 nm). Electrical conductivity and Seebeck coefficient of the films were measured in the temperature range 300–520 K, respectively employing the four probe and differential methods, using a commercial tester (RZ2001i, Ozawa Sciences). Electrical conductivity was measured first, at any temperature, followed by Seebeck coefficient, by introducing a temperature gradient (0–10 K, using which, periodic test measurements with Ni foils have always yielded data matching excellently with those reported by Burkov *et al.*[30] The properties at higher temperatures were measured by uniformly heating the film placed in the furnace.

3. Results and Discussion

The AFM images of untreated and acid-treated PEDOT:PSS films are shown in Figure 1. Untreated PEDOT:PSS films were smooth, with typical rms roughness of 2.4 nm as shown in Fig. 1(a). Significant changes in the AFM topography were observed after acid bath treatment for 15 minutes as shown in Fig. 1(b). Acid treatment is expected to remove the PSS domains, causing the morphological changes. The increased rms roughness up to 3.5 nm and growth of small fibrous structures is clearly evident from the topography and phase images. Further, extended bath treatment times of 2 and 4 h resulted in even more increased roughness of the films up to 4.4 nm as shown in Figs. 1(e) and 1(f). The corresponding phase images (Figs. 1(c, d, g and h)) also reveal the extended formation of fibrous structures after acid treatment. We have

confirmed through XRD analysis as shown in the supporting information, Fig. S1. It is clearly evident that acid treated film has a strong reflective peak at 2Θ = 6.2º, indicating the ordering or evolution of fibrous structures of PEDOT up on acid treatment while pristine PEDOT:PSS films exhibited amorphous structure. Further, the evolution of second order peak at 13.1º is a clear indication of possible lamella stacking between the two distinct alternating orderings of PEDOT and PSS. These kinds of observations are in coherence with the other literature reports.[31-33]

Upon acid treatment, some of the PSS^- ions get neutralized by the protons of H_2SO_4, causing the disappearance of Columbic attraction between PEDOT and PSSH as shown in the below equations.

$$H_2SO_4 \longrightarrow H^+ + HSO_4^- \quad p_{al}^k = -6.4 \ldots\ldots (I)$$

$$PSSH \longrightarrow PSS^- + H^+ \quad p_a^k = -2.8 \ldots\ldots (II)$$

Since p_{al}^k of H_2SO_4 is higher than p_a^k of PSSH, PSS^- units get protonated upon treatment with sulphuric acid. Hence, the overall reaction can be expressed as below:

$$H_2SO_4 + PSS^- \longrightarrow HSO_4^- + PSSH \ldots\ldots (III)$$

This will result into the replacement of PSS^- units by bisulfate ions as the counter ions for PEDOT grains. Neutral PSSH units can't exhibit Coulombic attractions with PEDOT grains, resulting in the phase segregation.

Figures 2 (a) and (b) show respectively the top and cross-sectional SEM images of the PEDOT:PSS films that has undergone acid treatment. Compared to the inset to Fig. 2(a), which represents the top view SEM image of untreated film, the emergence of a fibrous structure upon acid treatment is evident in Fig. 2(a). The surface morphology of the films before acid treatment is shown in the inset of Fig. 2(a). The cross sectional image shows that the fibrous nature is not

limited to the surface alone and the film appears to be porous (see Fig. 2(b)). Possible conformational changes as a result of the removal of PSS component is shown schematically in Fig. 2(c). Raman spectra for various PEDOT:PSS samples after acid treatment are compared with those of the untreated film as shown in Fig. 2(d). Since PSS is a weak Raman scatterer, all peaks are assigned to the various normal modes of vibration of atoms present in the PEDOT unit. The bands at higher wavenumbers such as 1573, 1503 cm^{-1} could be assigned to asymmetric stretching of $C_\alpha=C_\beta$ while the most intense peak at around 1440 cm^{-1} relates to symmetric stretching of $C_\alpha=C_\beta$ of five-membered thiophene ring. The peak at 1367 cm^{-1} corresponds to $C_\beta–C_\beta$ inter-ring stretching, 1264 cm^{-1} represents $C_\alpha–C_\alpha$ inter-ring stretching, 1105 cm^{-1} is due to C-O-C deformation, 988 cm^{-1} represents C-C anti-symmetrical stretching mode, 702 cm^{-1} corresponds to symmetric C-S-C deformation, 573 cm^{-1} due to oxy-ethylene ring deformation and 441 cm^{-1} correspond to SO_2 bending, confirms the doping of sulfate and bisulfate anions (from sulphuric acid) in PEDOT. The reference spectrum has a peak at 441 cm^{-1} which can be ascribed to the doping of PEDOT by the SO_3^- ion from PSS units. It should be noted that even for the untreated PEDOT:PSS films, doping of sulfite groups is caused from the PSS units. Hence, we do observe the 441 cm^{-1} band in either of the samples (untreated as well as acid treated PEDOT:PSS films). The shift in the position of C=C (1438 cm^{-1}) towards higher wavenumbers (see Fig. 2(e)) up on acid treatment is due to increased doping of PEDOT:PSS by bisulfate anions. Untreated PEDOT:PSS film shows the stretching vibration at 1438 cm^{-1}, which gets shifted to 1451.15 cm^{-1} for 4 h bath treated film. Several groups have also observed the similar shift, attributed to the doping of PEDOT by either chemical or electrochemical manner.[34,35] This conducting mechanism is associated with an increase of doping up on acid treatment that can be explained as follows. In the case of untreated PEDOT:PSS films, the

amount of doping can be caused by the uni-negatively charged ions SO_3^- (from PSS segments) to create polarons or sometimes bipolaron carriers (maybe caused by excess HSO_4^- compared to PSS^-) in the PEDOT backbone. Thus, the acid treatment is helping to increase the doping level in PEDOT and hence enhanced electrical conductivity.[35] A 50-fold decrease in impedance is observed in the acid-treated films as compared to the films untreated with acid, as shown in the Bode plots shown in Fig. 3. The decrease in impedance is concluded to be a direct consequence of improved electrical conductivity, supporting the hypothesis of removal of PSS components from the acid-treated films.

In order to confirm the removal of PSS from the films upon acid treatment, few of the films were also subjected to UV-Vis Spectroscopy analysis, the result of which is shown in Fig. 4. It is seen that the absorbance shoulder peak at around 225 nm and the overall absorbance of the films reduced, with increase in acid treatment duration, as compared to the untreated film. The characteristic absorbance shoulder peak arises from the aromatic ring of the PSS components[36] and the removal of PSS results in the enhanced transparency of the films, as reported elsewhere.[37]

The temperature dependence of electrical conductivity of the films is shown in Fig. 6 (a). All the films show a metal-like behavior, with electrical conductivity decreasing with increase in temperature, indicating that the carrier density in the films is high. The metal-like conduction is believed to be the dominant conduction mechanism in the temperature range of interest. Broadly, for lightly or moderately doped conjugated polymers, variable-range hopping dominates the conduction in the semiconductor regime of the semiconductor-metal transition, once localized states are formed in the band gap. It has been established[38] that the inherent low dimensional nature, of the constituent molecules of conjugated polymers such as PEDOT:PSS, is not a

hindrance in achieving metal-like conductivity in these systems, since the electronic structure of such polymers can indeed resemble that of a disordered metal. The overlap of wave functions can occur in heavily doped conducting polymers. The effect of acid treatment is strikingly evident, from the enhancement in electrical conductivity as a result of the removal of PSS components in the films. Once PSS is slowly removed from the films, the conductivity is expected to be enhanced by (i) elongation and alignment of PEDOT chains and (ii) the reduction in density of the amorphous PSS regions. In such a series heterogeneous model of a conducting polymer with higher (PEDOT) and lower (PSS) conductivity constituents connected electrically in series, the total resistivity can be written as[39] $\rho\ (T) = \sum_i f_i \rho_i\ (T)$, where f_i is the geometric factor given by $f_i = \frac{L_i A}{L A_i}$, L and A being the total effective length and cross-sectional area of the sample while $L_i$and A_i are the length and cross-sectional area of a constituent material i with intrinsic resistivity $\rho_i\ (T)$. In such a heterogeneous model, with increase in concentration of the conducting constituent as opposed to the non-conducting constituent, the overall conductivity becomes

$$\sigma\ (T) = 1/\rho(T) \approx\ \sigma_1(T)/f_1 \ldots\ldots (\mathrm{IV})$$

where $\sigma_1(T)$ and f_1 are the conductivity and geometric factor of the highly conducting constituent. The observed increase in conductivity of PEDOT:PSS films can then be explained by considering the relative increase in area of cross section of the conducting PEDOT chains as opposed to the insulating PSS shells throughout the cross-section of the films, upon removal of PSS during acid treatment. As evident from Fig. 5a, electrical conductivity increases with the acid treatment time, suggesting that PSS is removed continuously from the film during the entire duration of the acid treatment. Moreover, the conformation changes brought in by the removal of

PSS cause delocalization of positive charges, which also contribute to the enhanced conductivity. Our attempts at increasing the acid treatment time beyond 4 h were unsuccessful since the films either became wrinkled or entirely peeled off from the substrate.

Another important consequence of considering a series heterogeneous model as described above is the possible metal-like conductivity at high temperatures, similar to what is observed in other polymers such as polyacetylene and polyaniline.[39] For extended metallic regions with intermediate insulating boundaries, the total conductivity which is due to a combination of quasi 1-D metallic conductivity and a temperature assisted tunneling process, where the former decreases and the latter increases with temperature, can be expressed as[39]

$$\sigma(T) = (\rho(T))^{-1} = (f_1\rho_m \exp\left(\frac{-T_m}{T}\right) + f_2\rho_t \exp\left(\frac{-T_t}{T+T_s}\right))^{-1} \quad \ldots\ldots (V)$$

where f_1 and f_2 are the geometric factors of the conducting and insulating regions, ρ_m and ρ_t are the metallic and tunneling pre-factors, T_t is the temperature at electronic energy states are raised over the barrier due to the large thermal voltage fluctuations and the ratio T_t/T_s determines the tunneling in the absence of fluctuations. Excellent fits could be obtained for the temperature dependent conductivity curves using the above expression, as shown by red lines in Fig. 6a. The fitting parameters are shown in Table 1. It is interesting to note that the geometric factor f_1 (f_2) progressively increases (decreases) with increase in acid treatment time, which further supports the idea that PSS is removed from the films upon acid treatment.

The Seebeck coefficient and power factor of the films as a function of temperature are shown in Figs. 5(b) and 5(c) respectively (see Fig. S2). The Seebeck coefficient of the films increases almost linearly with temperature up to around 460 K. Such a linear temperature

dependence further supports the metal-like nature of electronic transport in PEDOT:PSS and the ideal metallic diffusion thermopower, for conduction involving states close to the Fermi level, may be expressed as[40]

$$S = \frac{\pi^2 k_B^2 T}{3e} \left. \frac{\partial \ln \sigma(E)}{\partial E} \right|_{E_F} , \ldots\ldots \text{(VI)}$$

where $\sigma(E)$ is the conductivity the material would have if the Fermi level E_F were at electron energy E, k_B is the Boltzmann constant and e is the charge of electron.

It is seen that acid treatment enhances not only the electrical conductivity of the films, but the Seebeck coefficient as well, which in turn results in improvement of power factor. The simultaneous increase in electrical conductivity and Seebeck coefficient is interesting, since in conventional thermoelectric materials, the two properties are often inversely related. From our studies, it is evident that acid treatment results in the removal of PSS and hence it should be concluded that PSS acts as a barrier for the transport of holes through the polymer network. The extended conjugated PEDOT chains, which form after the removal of PSS, act as a high mobility path for the transport of electrons. The result is an enhancement in electrical conductivity. The removal of PSS may also alter the local band structure of PEDOT:PSS. It is evident that such a possible change in band structure may be responsible for the observed enhancement in Seebeck coefficient. The film exposed to acid treatment for 4 h shows a 5-fold increase in power factor at 460 K, compared to the untreated film. The huge surge in power factor upon acid treatment is both significant and encouraging, for further advancement of organic thermoelectrics. Beyond 460 K, it is observed that the Seebeck coefficient starts to decrease. A close observation of the electrical conductivity of the films shows a change in slope of the conductivity curves around this temperature. Also, when films heated beyond 460 K are cooled, the electrical conductivity

showed a hysteresis (not shown), while no such hysteresis was observed for films heated only up to 460 K. Hence, it is clear that beyond 460 K, there are irreversible changes in the film and the highest temperature of stable operation is around 460 K.

4. Conclusions

In conclusion, it has been shown that acid treatment of PEDOT:PSS thin films induces simultaneous increase in electrical conductivity and Seebeck coefficient. The thermoelectric power factor of the acid-treated films increases with temperature up to 460 K, with a peak power factor of 0.052 W/m. K. This value is five times higher than the corresponding value of untreated PEDOT:PSS films. The enhancement is attributed to the loss of PSS from the PEDOT:PSS films besides the morphology change in the PEDOT grains, which enhances hole transport and is believed in modifying the local band structure of the material, simultaneously increasing the Seebeck coefficient.

Acknowledgement

The authors acknowledge the financial support provided by King Abdullah University of Science and Technology (KAUST), Saudi Arabia for carrying out this work.

References

1. O. Inganas, Nat Photon 5 (4), 201-202 (2011).
2. Q. Zhang, Y. Sun, W. Xu and D. Zhu, Advanced Materials, n/a-n/a (2014).
3. G. H. Kim, L. Shao, K. Zhang and K. P. Pipe, Nat Mater 12 (8), 719-723 (2013).
4. A.-D. Bendrea, L. Cianga and I. Cianga, Journal of Biomaterials Applications 26 (1), 3-84 (2011).
5. A. B. Kaiser, Advanced Materials 13 (12-13), 927-941 (2001).
6. P.-C. Wang, L.-H. Liu, D. Alemu Mengistie, K.-H. Li, B.-J. Wen, T.-S. Liu and C.-W. Chu, Displays 34 (4), 301-314 (2013).
7. R. A. Green, S. Baek, L. A. Poole-Warren and P. J. Martens, Science and Technology of Advanced Materials 11 (1), 014107 (2010).

8. A. Ramanavičius, A. Ramanavičienė and A. Malinauskas, Electrochimica Acta 51 (27), 6025-6037 (2006).
9. G. A. Snook, P. Kao and A. S. Best, Journal of Power Sources 196 (1), 1-12 (2011).
10. N. Dubey and M. Leclerc, Journal of Polymer Science Part B: Polymer Physics 49 (7), 467-475 (2011).
11. M. Leijnse, K. Flensberg and T. Bjørnholm, in *Organic Optoelectronics* (Wiley-VCH Verlag GmbH & Co. KGaA, 2013), pp. 467-486.
12. X. Gao, K. Uehara, D. D. Klug, S. Patchkovskii, J. S. Tse and T. M. Tritt, Physical Review B 72 (12), 125202 (2005).
13. M. He, F. Qiu and Z. Lin, Energy & Environmental Science 6 (5), 1352-1361 (2013).
14. O. Bubnova and X. Crispin, Energy & Environmental Science 5 (11), 9345-9362 (2012).
15. Y. Du, S. Z. Shen, K. Cai and P. S. Casey, Progress in Polymer Science 37 (6), 820-841 (2012).
16. J. Luo, D. Billep, T. Waechtler, T. Otto, M. Toader, O. Gordan, E. Sheremet, J. Martin, M. Hietschold, D. R. T. Zahn and T. Gessner, Journal of Materials Chemistry A 1 (26), 7576-7583 (2013).
17. O. Bubnova, Z. U. Khan, A. Malti, S. Braun, M. Fahlman, M. Berggren and X. Crispin, Nat Mater 10 (6), 429-433 (2011).
18. T.-C. Tsai, H.-C. Chang, C.-H. Chen and W.-T. Whang, Organic Electronics 12 (12), 2159-2164 (2011).
19. A. Kim and S. Greg, in *Polymer Composites for Energy Harvesting, Conversion, and Storage* (American Chemical Society, 2014), Vol. 1161, pp. 147-163.
20. S. K. Yee, N. E. Coates, A. Majumdar, J. J. Urban and R. A. Segalman, Physical Chemistry Chemical Physics 15 (11), 4024-4032 (2013).
21. B. Zhang, J. Sun, H. E. Katz, F. Fang and R. L. Opila, ACS Applied Materials & Interfaces 2 (11), 3170-3178 (2010).
22. W. Qingshuo, M. Masakazu, K. Kazuhiro, N. Yasuhisa and I. Takao, Applied Physics Express 7 (3), 031601 (2014).
23. N. Massonnet, A. Carella, O. Jaudouin, P. Rannou, G. Laval, C. Celle and J.-P. Simonato, Journal of Materials Chemistry C 2 (7), 1278-1283 (2014).
24. S. Liu, H. Deng, Y. Zhao, S. Ren and Q. Fu, RSC Advances 5 (3), 1910-1917 (2015).
25. J. Ouyang, ACS Applied Materials & Interfaces 5 (24), 13082-13088 (2013).
26. Y. Xia, K. Sun and J. Ouyang, Advanced Materials 24 (18), 2436-2440 (2012).
27. D. A. Mengistie, C.-H. Chen, K. M. Boopathi, F. W. Pranoto, L.-J. Li, and C.-W. Chu, *ACS Appl. Mater. Interfaces*, 7 (1), 94–100 (2015)
28. J. Wang, K. Cai and S. Shen, Organic Electronics 15 (11), 3087-3095 (2014).
29. I. Horcas, R. Fernández , J. M. Gómez-Rodríguez , J. Colchero , J. Gómez-Herrero , A. M. Baro , *Rev. Sci. Instrum*, 78, 013105 (2007).
30. A. T.Burkov, A. Heinrich, P. P. Konstantinov, T. Nakama, K. Yagasaki, *Measure. Sci. Technol., 12*, 264–272 (2001).
31. M. V. Fabretto D. R. Evans, M. Mueller, K. Zuber, P. Hojati-Talemi, R. D. Short, G. G. Wallace and Peter J. Murphy, *Chem. Mater.*, 24, 3998 (2012).
32. M. A. Ali, H. Kim, C. Lee, H. Nam, J. Lee, *Synth. Met.* 161, 1347 (2011).

33. N. Kim, S. Kee, S. H. Lee, B. H. Lee, Y. H. Kahng, Y.-R. Jo, B.-J. Kim and K. Lee, Adv. Mater., 26, 2268 (2014).

34. W. W. Chiu, J. Travaš-Sejdić, R. P. Cooney and G. A. Bowmaker, Synthetic Metals 155 (1), 80-88 (2005).
35. M. Reyes-Reyes, I. Cruz-Cruz and R. López-Sandoval, The Journal of Physical Chemistry C 114 (47), 20220-20224 (2010).
36. A. K. Sarker, J. Kim, B.-H. Wee, H.-J. Song, Y. Lee, J.-D. Hong and C. Lee, RSC Advances 5 (64), 52019-52025 (2015).
37. T. Koyama, T. Matsuno, Y. Yokoyama and H. Kishida, Journal of Materials Chemistry C 3 (32), 8307-8310 (2015).
38. A. N. Aleshin, Phys. Solid State 52 (11), 2307-2332 (2010).
39. A. B. Kaiser, Reports on Progress in Physics 64 (1), 1 (2001).
40. N. Mott and E. Davis, (Oxford, 1979).

Table 1. Parameters used for fitting the electrical conductivity data, using equation (2), as shown in Fig.3. For details, please refer text

Film	f_1	f_2	ρ_m ($\times$ 10^{-3} Ω cm)	ρ_t ($\times$ 10^{-4} Ω cm)	T_m (K)	T_t (K)	T_s (K)
Untreated	0.55	0.45	2.02	1.12	300	50	20
Acid-treated (15 m)	0.90	0.10	1.13	8.01	300	50	20
Acid-treated (2 h)	0.91	0.09	1.10	7.40	290	50	20
Acid-treated (4 h)	0.93	0.07	0.92	4.45	290	50	20

Figures

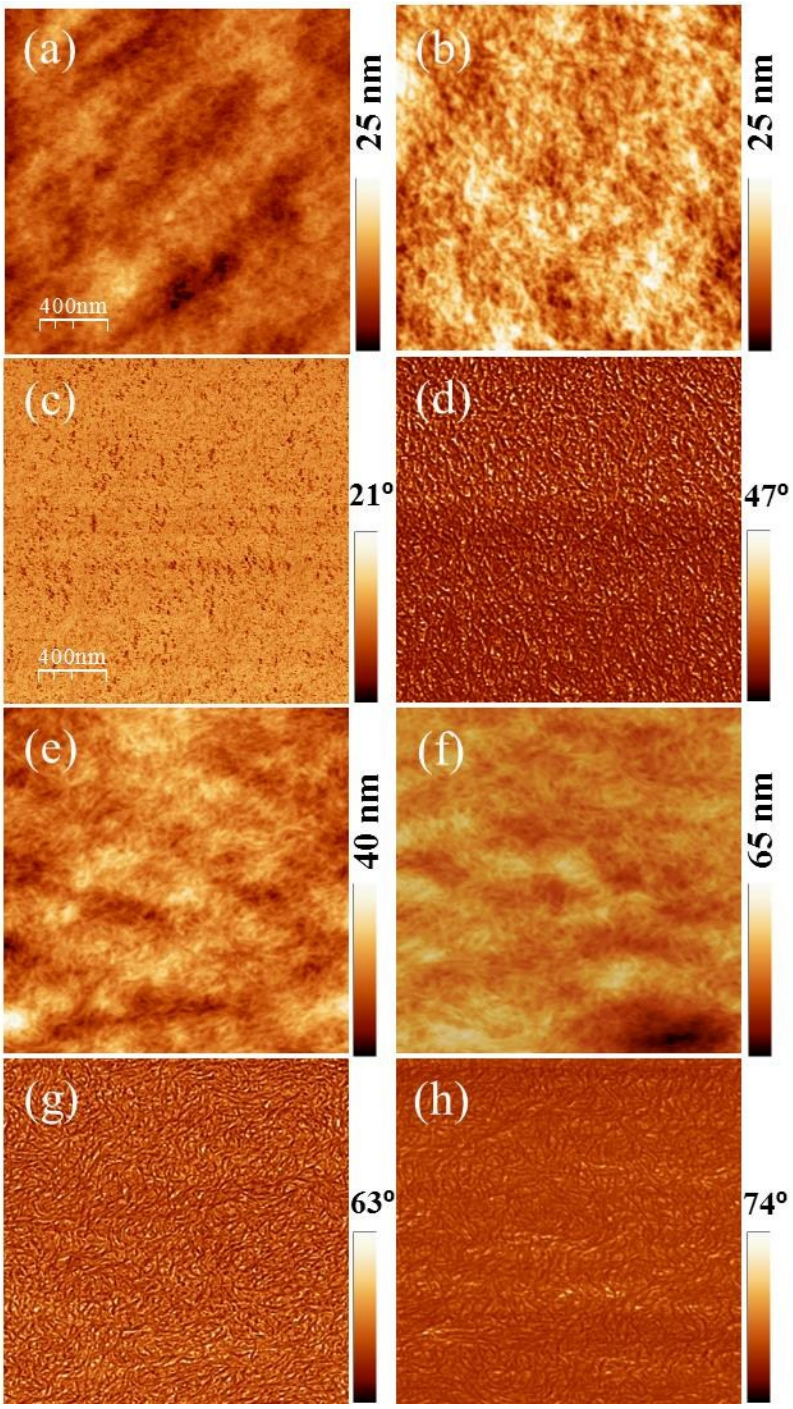

Fig. 1. AFM topography images of (a) pristine and bath treated PEDOT:PSS films for (b) 15 min, (e) 2 h and (f) 4 h, corresponding phase images are shown in the immediate below panels (c, d, g, h). The scan size for each image is 2x2 μm. Corresponding z-scales are shown for each image.

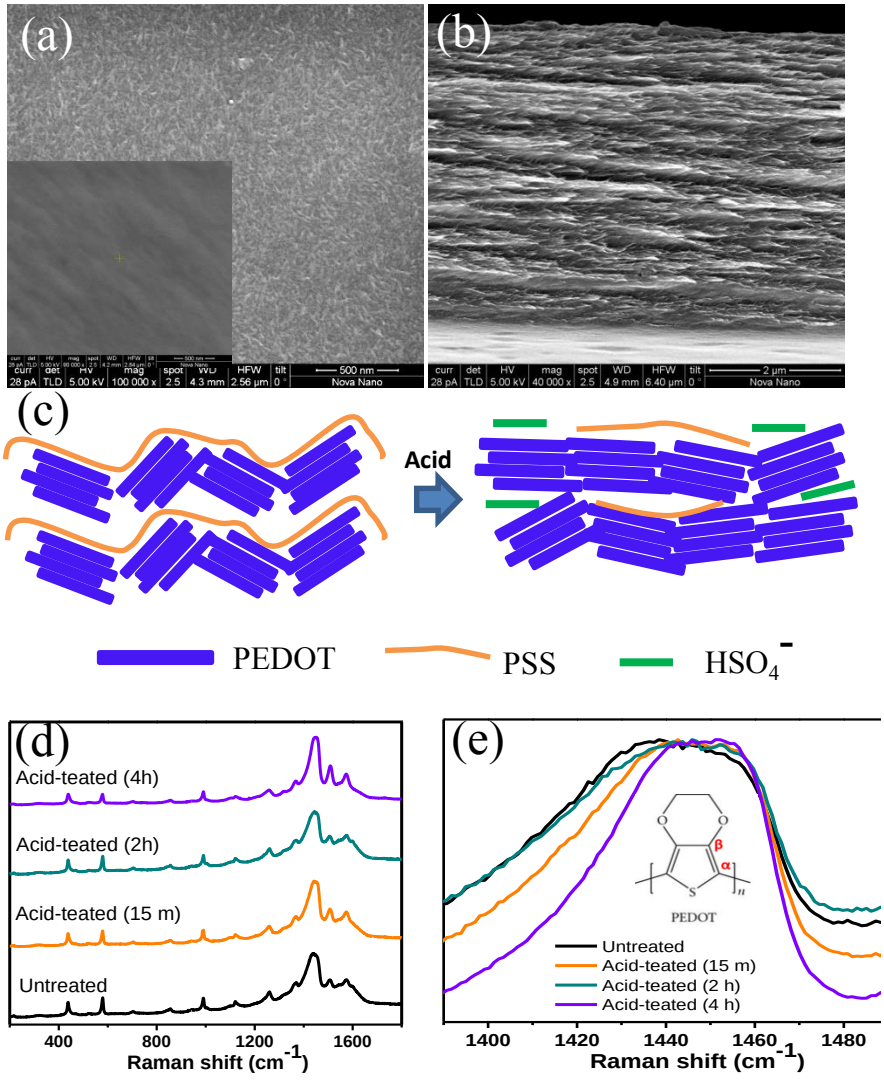

Fig.2. Representative SEM micrographs of PEDOT:PSS films after acid treatment (a) top and (b) cross-sectional views, inset shows the plane view of untreated film. (c) schematic depicting the possible conformational changes in the PEDOT chains up on acid treatment, (d) comparative Raman spectra of untreated PEDOT:PSS with respect to acid treatment for different times and (e) Raman spectra showing the shift in the symmetric stretching of $C_\alpha = C_\beta$ vibration up on acid treatment.

Fig. 2

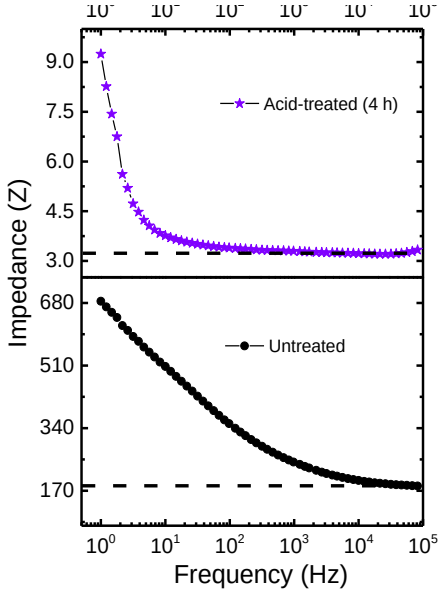

Fig.3. Bode (Impedance vs. Frequency) plots for the untreated and acid-treated PEDOT:PSS films.

Fig. 3

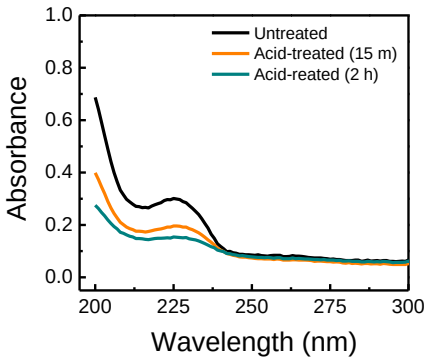

Fig.4. Comparison of UV absorption of untreated and acid treated PEDOT:PSS films.

Fig. 4

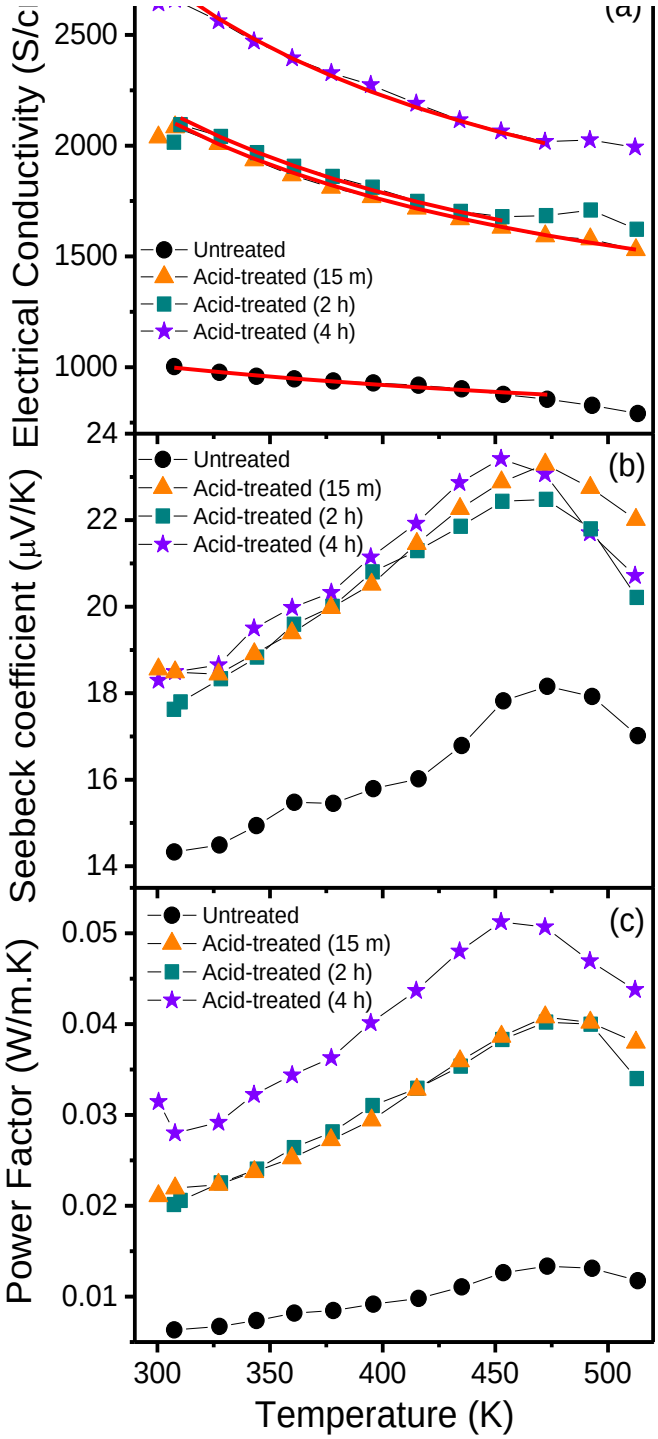

Fig.5. Temperature dependence of (a) electrical conductivity, (b) Seebeck coefficient and (c) power factor of untreated and acid-treated PEDOT:PSS films. Red lines represent the fitted curves using equation (2).

Fig. 5

ToC

Enhanced thermoelectric response of acid treated conducting polymer thin films.